Post-jökulhlaup geomorphic evolution of the Gígjökull Basin, Iceland

D. Harrison [ID], N. Ross [ID], A. J. Russell and S. A. Dunning

School of Geography, Politics and Sociology, Newcastle University, Newcastle upon Tyne, UK

Abstract

How landscapes respond to, and evolve from, large jökulhlaups (glacial outburst floods) is poorly constrained due to limited observations and detailed monitoring. We investigate how melt of glacier ice transported and deposited by multiple jökulhlaups during the 2010 eruption of Eyjafjallajökull, Iceland, modified the volume and surface elevation of jökulhlaup deposits. Jökulhlaups generated by the eruption deposited large volumes of sediment and ice, causing significant geomorphic change in the Gígjökull proglacial basin over a 4-week period. Observation of these events enabled robust constraints on the physical properties of the floods which informs our understanding of the deposits. Using ground-based LiDAR, GPS observations and the satellite-image-derived ArcticDEMs, we quantify the post-depositional response of the 60 m-thick Gígjökull sediment package to the meltout of buried ice and other geomorphic processes. Between 2010 and 2016, total deposit volume reduced by $-0.95 \times 10^6 \, \mathrm{m^3 \, a^{-1}}$, with significant surface lowering of up to 1.88 m a^{-1}. Surface lowering and volumetric loss of the deposits is attributed to three factors: (i) meltout of ice deposited by the jökulhlaups; (ii) rapid melting of the buried Gígjökull glacier snout; and (iii) incision of the proglacial meltwater system into the jökulhlaup deposits.

Introduction

It has been hypothesised that an increase in subglacial eruptions and their consequent jökulhlaups (glacial outburst floods) could result from a deglaciation-driven glacio-isostatic response of the Earth's mantle (Pagli and Sigmundsson, 2008; Carrivick and others, 2009). If correct, this process would increase the already high potential for volcano–ice interactions within Iceland, given that over 60% of Icelandic ice masses overlie active volcanic zones (Björnsson, 2002). Understanding the response of the landscape following deposition from large outburst floods is a vital step for assessing future jökulhlaup routing and the identification of jökulhlaup hazard potential (Cassidy and others, 2003; Duller and others, 2008). Burial of glacier ice, and deposition of jökulhlaup-transported ice (from ice blocks to sediment–ice slurries), occurs frequently during jökulhaups (Fay, 2002a,2002b; Burke and others, 2010). The meltout of buried ice masses, following jökulhlaup deposition, can lead to widespread surface lowering and the formation of kettle holes (Maizels, 1992).

The 2010 eruption of Eyjafjallajökull (14 April to 22 May) generated numerous jökulhlaups that inundated the Gígjökull proglacial basin (Fig. 1), infilling it with large volumes of sediment and ice (Magnússon and others, 2012). The two highest magnitude floods occurred during 14–16 April, with peak discharges of up to 2700 m^3 s^{-1} and a combined volume of flood water totalling 57×10^6 m^3 (Magnússon and others, 2012). Over 140 smaller jökulhlaups were recorded during the rest of the eruption, with discharges between 10 and 226 m^3 s^{-1} and water volumes up to 3×10^6 m^3 (Dunning and others, 2013). Following the eruption and jökulhlaups, the Gígjökull basin was characterised by a ~60 m-thick sequence of coarse fluvioglacial sediment and flood-transported glacier ice, underlying a steeply-sloping progradational fan surface (Fig. 2) (Dunning and others, 2013). Initial estimates indicated a total deposited sediment volume of ~17 × 10^6 m^3, although the partitioning between sediment and ice within the deposit is uncertain (Dunning and others, 2013). Field observations at the time of deposition indicate a composition of up to 80% ice for deposits associated with the jökulhlaup on the 15 April 2010.

The post-eruption morphology and surface sedimentology of the proximal Gígjökull basin were predominantly the result of the lower discharge jökulhlaups during the later stages of the event (Dunning and others, 2013). This is in contrast to the common understanding of volcanogenic jökulhlaups, with geomorphic and sedimentological signatures formerly attributed to peak sediment flux coincident with peak discharge from a single hydrograph, and little to no deposition during the waning stages (Maizels, 1997; Russell and others, 2010). These later smaller jökulhlaups were only responsible for ~15% of the basin infill, but were a dominant mechanism for the present-day surface morphology of the proximal part of the Gígjökull basin and most of the near-surface sedimentology (Dunning and others, 2013).

Aims

In this study, we investigate the role of geomorphic processes, including jökulhlaup transported ice, buried glacier ice and fluvial incision, in the post-depositional modification of jökulhlaup deposits. Dunning and others (2013) investigated the immediate post-eruption
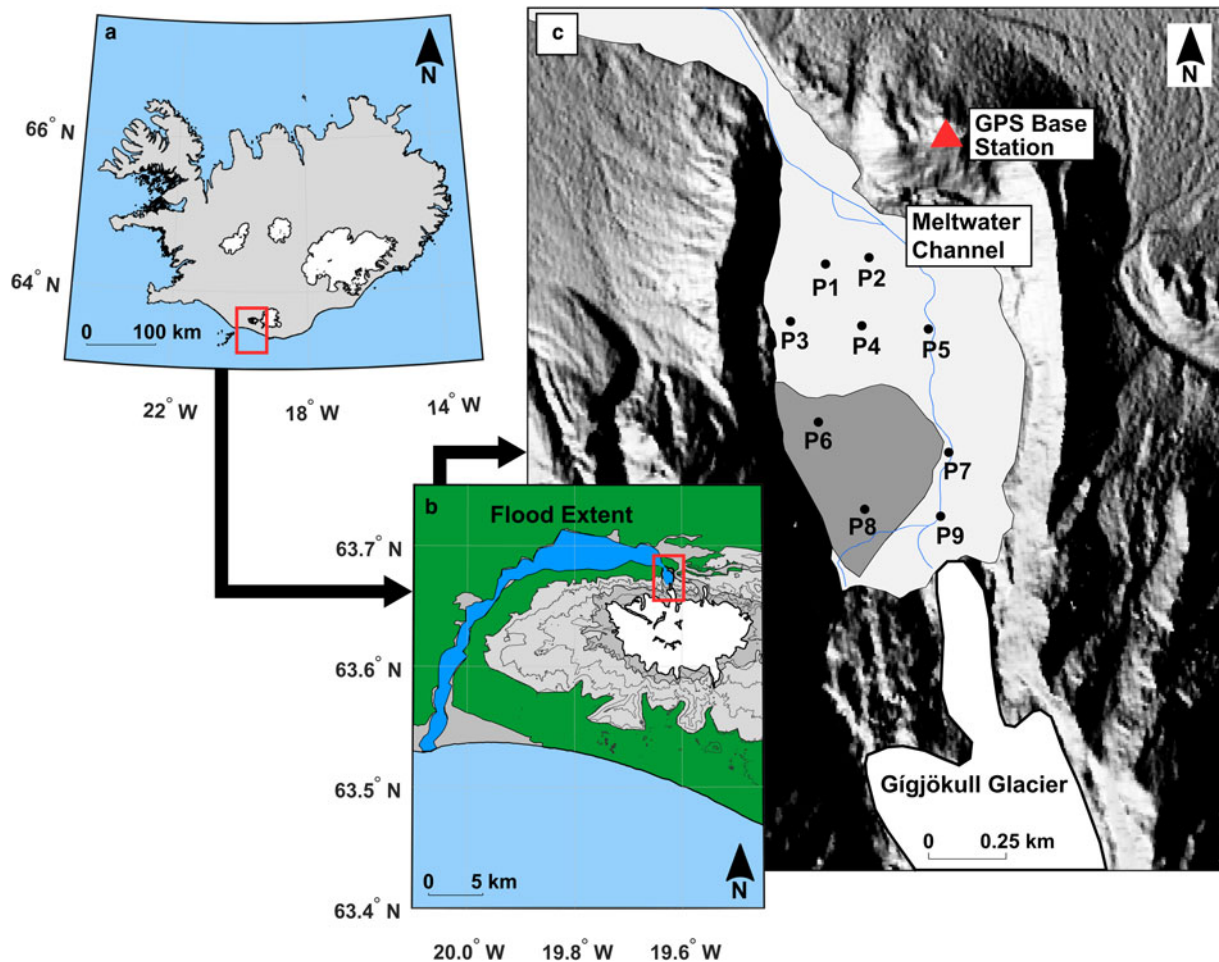
Fig. 1. Location map of the Gígjökull basin, Iceland. (a) Map of Iceland showing the largest ice caps. Location of the Eyjafjallajökull ice cap highlighted by the red box. (b) Eyjafjallajökull ice cap and the Markarfljót fluvial system. Blue polygon shows the extent of the 2010 jökulhlaups from source to sea. Location of the Gígjökull basin highlighted by red box (extent of Figs 2 and 5). (c) The Gígjökull basin. Ice-proximal fan shown by dark grey polygon. P1–P9 represent point elevation measurement locations.

evolution of the deposits, but that analysis was temporally limited to March–July 2010. Here we extend that analysis to determine the evolution of the Gígjökull basin over a 6-year period from 2010 to 2016. The active observations and robust constraints on the physical properties of the 2010 floods provide a unique opportunity to inform our understanding of the subsequent deposits and their evolution. We undertake the first systematic survey of post-depositional modification of recently emplaced jökulhlaup deposits, using repeated field surveys (e.g. TLS and dGPS) and remotely sensed datasets (e.g. ArcticDEM) to characterise surface elevation change over a 6-year period (2010–2016).

Study area

Located in south central Iceland (Fig. 1a), the Eyjafjallajökull ice cap covers an area of 67 km^2 and like many Icelandic glaciers has decreased in size, in this case by 0.3–0.5% each year (Sigurðsson and others, 2017). Ice thickness varies from 100 m on the slopes, to ∼200 m on the summit caldera of the Eyjafjallajökull stratovolcano (Sturkell and others, 2010; Magnússon and others, 2012). Gígjökull is the largest outlet from the Eyjafjallajökull ice cap (Sturkell and others, 2010) (Fig. 1c). Prior to the eruption of Eyjafjallajökull, Gígjökull terminated in the 20–30 m deep Gígjökulslón proglacial lake, surrounded by a bedrock and moraine ridge complex up to 70 m in height (Spedding, 2000; Kirkbride and Dugmore, 2008; Magnússon and others, 2012).

The Gígjökull proglacial basin is a glacial overdeepening formed during periods of advanced terminus position of Gígjökull (Spedding, 2000). The basin is positioned on the eastern end of the Markarfljót sandur, and is a tributary valley of the Markarfljót braided river system (Snorrason and others, 2012).

Methods

Differential GPS (dGPS) survey

Extensive dGPS surveys of the Gígjökull basin were conducted during 19–21 June 2015 and 22 September to 1 October 2016 using Leica Viva GS14 Global Navigation Satellite Systems (GNSS). Two systems were deployed in the basin, utilising one as a base station and the other as a rover unit for collecting point data. The survey was conducted in Real Time Kinematic (RTK) mode allowing for horizontal accuracies up to 1 cm and vertical accuracies of up to 10 cm. Due to the high number of data points collected in 2016 (∼4000) it was possible to create a digital elevation model (DEM) through interpolation processes (Arun, 2013). The topo2raster tool (Arun, 2013) was used to convert the data points to a DEM. A low-pass filter was then applied to the DEM, combined with a resampling function to create a raster with 5 × 5 m cell size. This smoothed the surface, removing any residual artefacts produced by the interpolation process. Data were then combined with the 2010 TLS-derived DEM
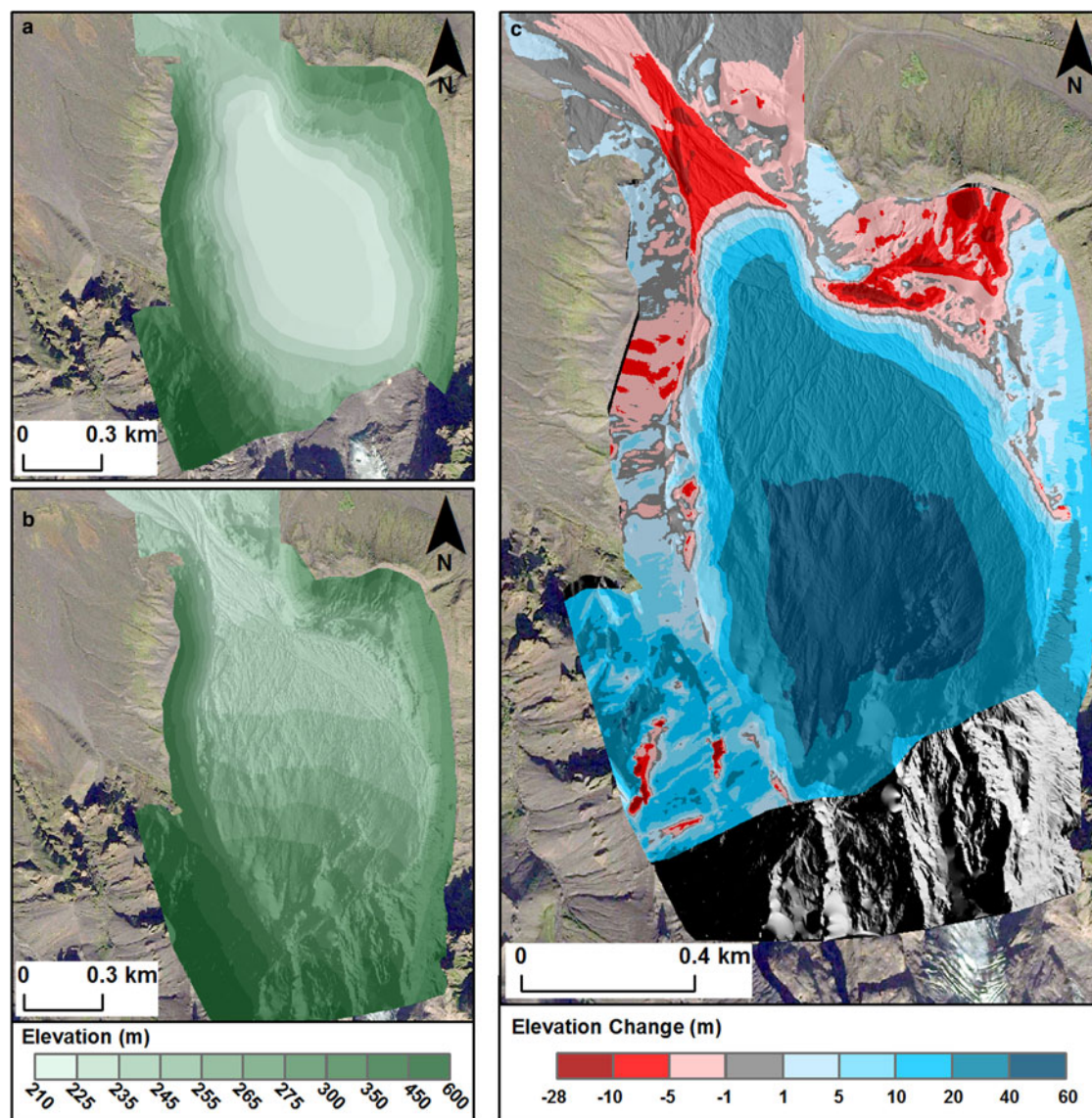
Fig. 2. Terrestrial Laser Scanner (TLS) derived DEM(s) collected by Dunning and others (2013) of the Gígjökull basin underlain by a hillshade of the TLS data (elevation with reference to the WGS84 ellipsoid). Background image from DigitalGlobe via Google Earth (Imagery Date: 05/09/13). (a) Pre-jökulhlaup DEM collected in March 2010. (b) Post-jökulhlaup DEM collected in July 2010. (c) Surface elevation change from March 2010 to July 2010. Modified from Figure 3 in Dunning and others (2013).

information (Dunning and others, 2013) and dGPS data from June 2015 to determine surface elevation change since the 2010 jökulhlaups. Furthermore, we present the results from nine data points (using a combination of dGPS, ArcticDEM and TLS data) that are spatially and temporally representative of the geomorphic processes that influence surface elevation change within the Gígjökull basin.

ArcticDEM

The ArcticDEM dataset (Porter and others, 2018) enables quantification of the spatial and temporal evolution of Arctic glacial and proglacial systems. We analysed 2×2 m strip ArcticDEM data (2010–2016), derived from stereoscopic processing of DigitalGlobe's Worldview-1, Worldview-2 and Worldview-3 imagery (Noh and Howat, 2015; Porter and others, 2018). Initial geolocation of the ArcticDEMs may have systematic vertical and horizontal offsets of 3–5 m due to errors in the sensor model. A single control point from a dGPS survey can rectify these offsets, however (Dai and Howat, 2017). We used our

dGPS base station elevation measurements (Fig. 1c) to correct for the systematic vertical offsets in the ArcticDEM datasets, as we can assume little or no surface elevation change at the base station location over the period of investigation. DEM differencing and volumetric calculations were performed on corrected and clipped DEMs to quantify geomorphic change of the Gígjökull deposits. DEMs with reduced spatial coverage due to cloud cover were removed from the analysis.

Terrestrial laser scanning

Dunning and others (2013) provide a detailed description of the acquisition and processing of the terrestrial laser scanner (TLS) derived DEMs acquired in 2010. In summary, surveys were conducted both pre- (March 2010) and post-eruption (July 2010) using multiple scans collected using a Riegl Z620i TLS with a nominal 2 km range. The resultant data were aligned, then post-processed into DEMs with a 1 m spatial resolution, ensuring a high signal-to-noise ratio at the scales of interest (Dunning and others, 2013).
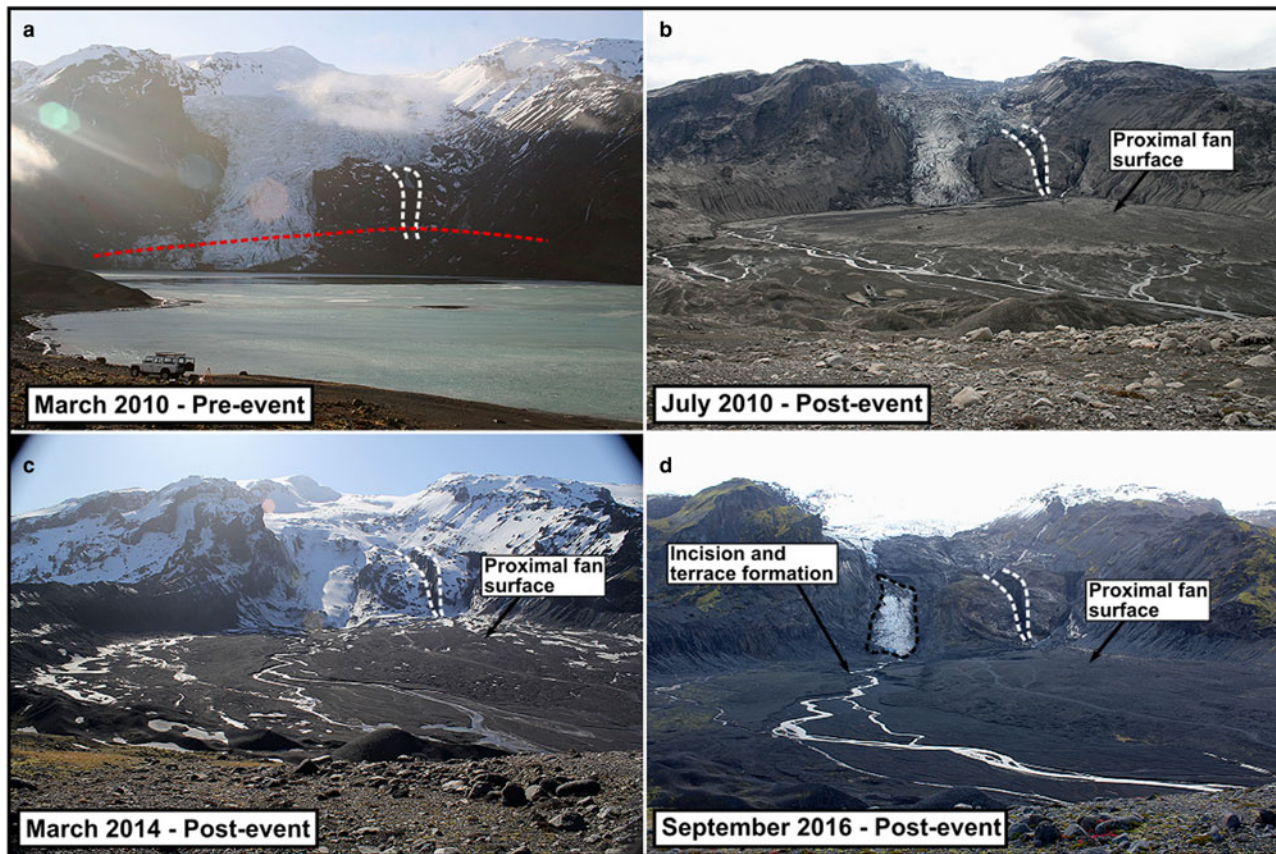
Fig. 3. Photo set showing the evolution of the Gígjökull basin from the pre-eruption landscape to the present day morphology. White dashed lines indicate jökulhlaup incised gorge (a–d). Red dashed line in (a) indicates jökulhlaup infill as of July 2010. Black dashed line in (d) shows the extent of the disconnected portion of Gígjökull outlet glacier. Photographs taken by Andrew J. Russell.

Ground-penetrating radar

We deployed an Utsi Groundvue 7 (GV7) low-frequency ground-penetrating radar (GPR) system (Francke and Utsi, 2009) at Gígjökull to collect large-scale sub-surface architectural profiles of jökulhlaup sediments (22 September to 1 October 2016). The GV7 system has a centre frequency of 40 MHz with an emitted bandwidth of 10–80 MHz (Francke and Utsi, 2009; Ross and others, 2018). Further technical specifications of the GV7 are described by Ross and others (2018). Over 40 km of radar lines were collected with multiple cross-sections collected perpendicular to jökulhlaup flow direction with a line spacing of ∼50 m. Key proximal-distal 'tie'-lines were also collected parallel to flow direction. Topographic information required for elevation correction during the processing of the resultant radargrams was gathered through a dGPS survey conducted coincident with the GPR survey. A velocity of 0.14 m ns^{-1} was used for the Gígjökull basin deposits, based upon a wide-angle reflection and refraction survey (WARR) (Harrison, 2018). Our recorded velocity value corresponds well with velocity values associated with unsaturated sands and gravels (Reynolds, 2011). Reflexw (http://www.sandmeier-geo.de/reflexw. html) geophysical processing and interpretation suite was used to process the radargrams. Processed radargrams were then imported into OpendTect (https://www.opendtect.org/) seismic interpretation software for 3D visualisation.

Results

Qualitative assessment of geomorphic change

The Gígjökull basin has experienced considerable geomorphological change as a result of the 2010 volcanogenic jökulhlaups (Fig. 3). During the study period (2010–2016), Gígjökull has receded and experienced ice mass loss (Figs 3a–d). The imagery shows increased exposure of the steep bedrock glacier bed and proglacial foreland at the glacier margins, illustrating the thinning of the glacier and the retreat of the terminus position. This vertical change is most pronounced between March 2010 and September 2016 (Figs 3a and d). Analysis of ArcticDEM datasets from 17 April 2010 to 30 November 2015 reveals that the glacier surface had lowered by up to 54 m and its margin has receded by roughly 150 m. The former glacier tongue has detached from the current main tongue of Gígjökull, leaving a lobe of stagnant ice on the slopes of Eyjafjallajökull (Fig. 3d). The extensive ice-proximal fan created during the smaller jökulhlaups (Dunning and others, 2013) underwent significant geomorphological change after jökulhlaup-related deposition on 16 May 2010. In July 2010, the fan was characterised by a smooth surface with an almost uniform gradient (Fig. 3b). The jökulhlaup deposits that formed the fan also led to the burial of the eastern portion of the glacier snout. The subsequent meltout of the buried glacier tongue produced large kettle holes in the most proximal parts of the Gígjökull basin (Fig. 4). By 2014, surface depressions were visible and the surface of the proximal fan displayed a pitted texture. The snow cover on the March 2014 photograph is useful in this instance as it emphasises depressions on the surface of the jökulhlaup deposits (Fig. 3c). Field observations reveal that these surface depressions are kettle holes likely to be the result of the meltout of buried ice blocks (Fig. 4). The proglacial stream, which flows across the basin from the glacier terminus and bedrock gorges to the Gígjökull moraines, also significantly incised the 2010 jökulhlaup deposits producing a series of well-defined terraces after May 2010 leading to the incision of the proximal fan.
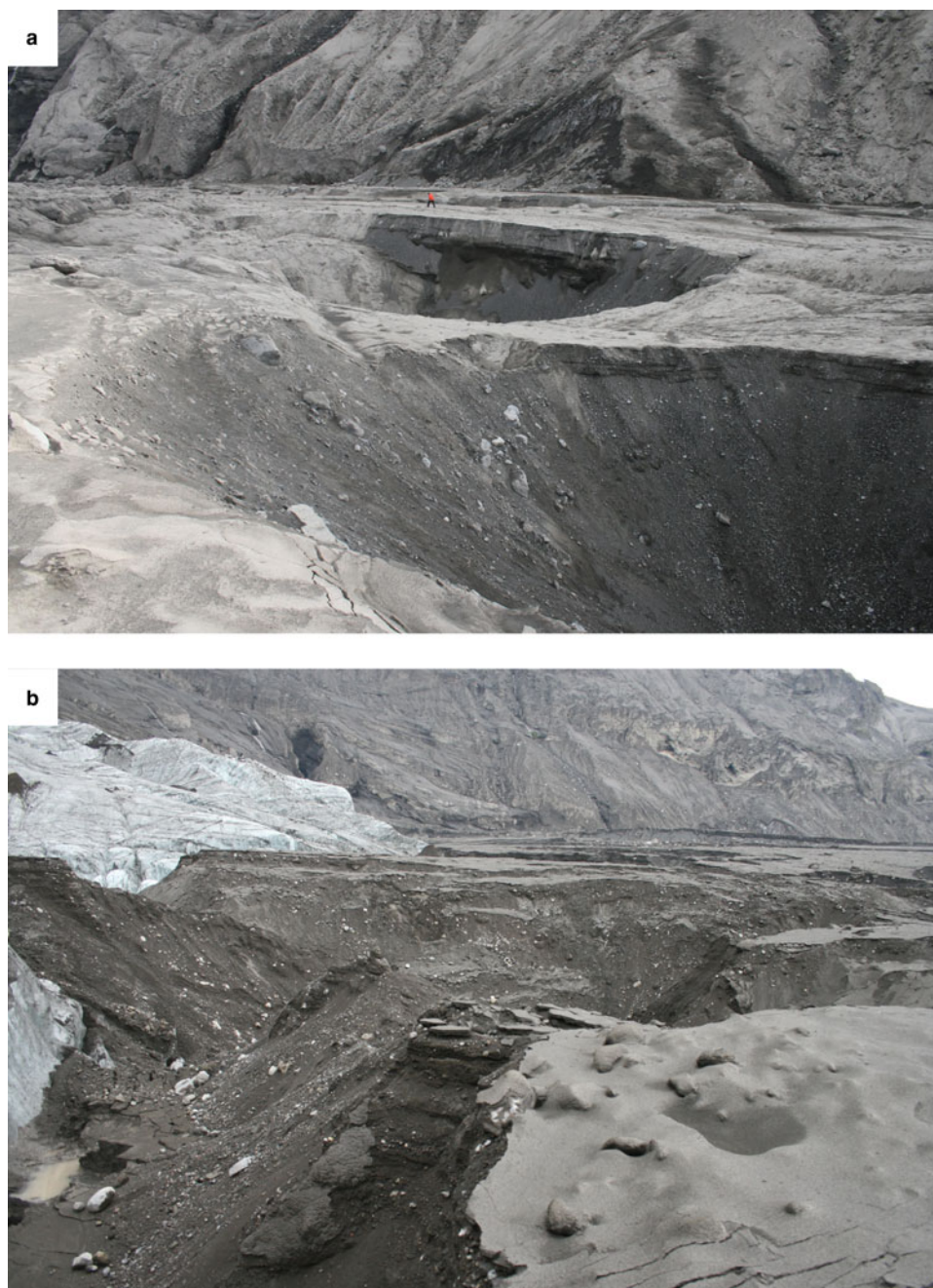
Fig. 4. (a) Development of large kettle holes by July 2010. Person in red jacket for scale. (b) Meltout of glacier snout buried by jökulhlaup deposits. Photographs taken by Andrew J. Russell.

Quantitative assessment of surface elevation change of the Gígjökull deposits

Jökulhlaup deposits within the Gígjökull basin experienced net surface lowering following the eruption from May 2010 to October 2016 (Fig. 5). A basin-wide surface lowering of the deposits, with an average of −1.75 m, is identifiable between May and July 2010. This is most likely a combination of sediment compaction and dewatering following the end of the jökulhlaups (Fig. 5c). Following this initial basin-wide change, surface lowering (May 2010 to September 2013) is focused in areas proximal to the post-jökulhlaup proglacial meltwater channel and the terminus of Gígjökull, with lowering of up to ∼20 m (Figs 5c and d). This lowering is predominately attributable to the meltout of glacier ice along the buried glacier margin in the eastern and central ice-proximal locations (Fig. 4), as well as meltwater channel incision, glacier terminus retreat and localised kettle hole development.

After September 2013, however, elevation change of the basin surface is no longer dominated by incision of the proglacial meltwater system and erosion of the jökulhlaup sediments in ice-proximal parts of the basin. The proximal fan displays areas of very limited elevation change (e.g. between −1 m and 1 m) during the period between 2013 and 2016. There are even small isolated areas of increased elevation, which are attributed to shadows in imagery used to produce ArcticDEM strips (Noh and Howat, 2015). By contrast, surface lowering in the more ice-distal locations of the basin occurs in a more widespread and uniform fashion (Figs 5d and e), with lowering ranging between 2 and 5 m during the periods of July 2010 to September 2013 (Fig. 5d), and September 2013 to October 2016 (Fig. 5e). Volume estimates calculated from the DEMs for the study period (i.e. March 2010 to October 2016) indicate that ∼26 × 10⁶ m³ of sediment and ice were deposited into the Gígjökull basin by the
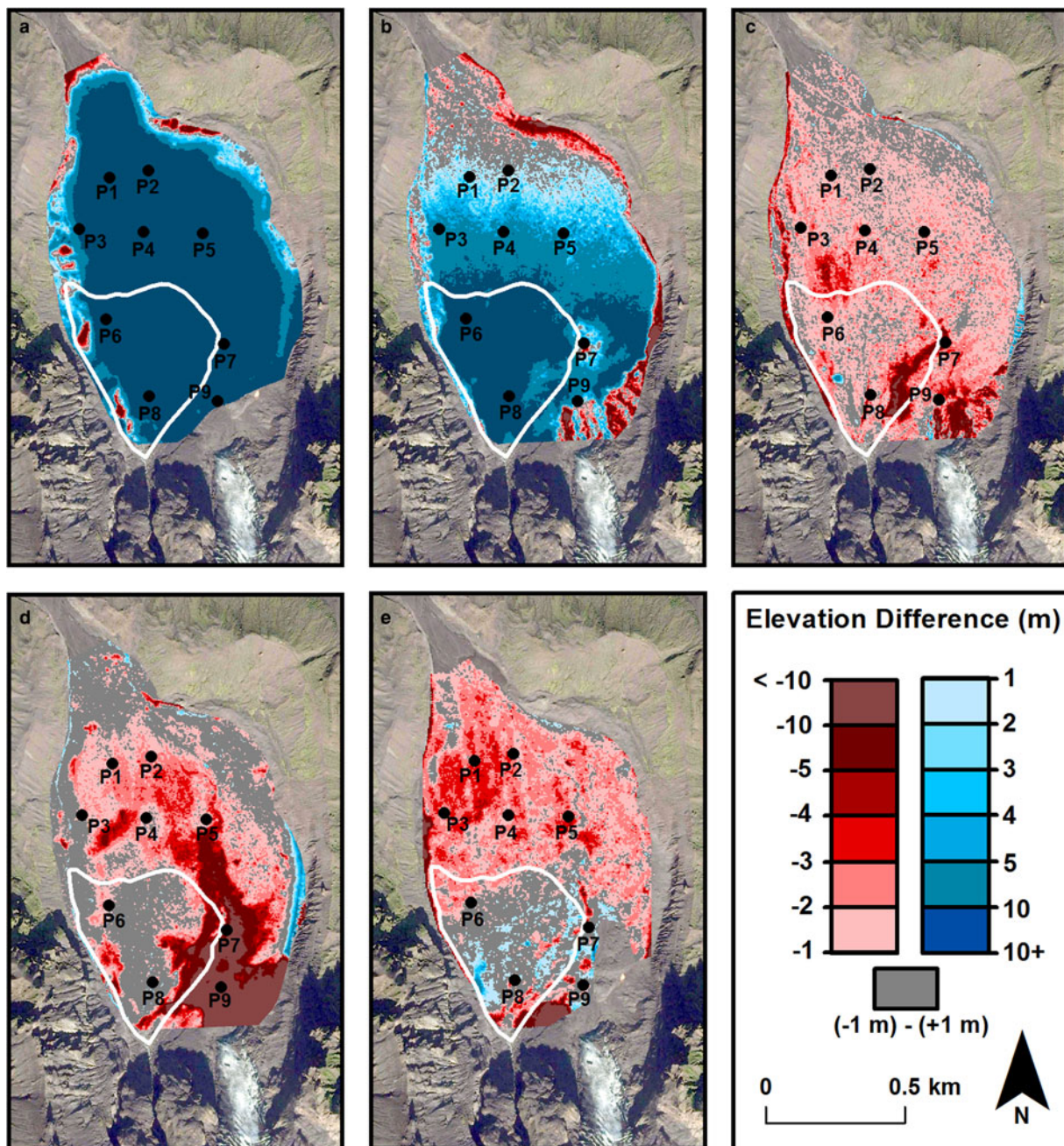
Fig. 5. DEMs of difference from comparison of TLS, ArcticDEM and dGPS datasets. White line indicates the extent of the ice-proximal fan as of September 2016. Background image from DigitalGlobe via Google Earth (Imagery Date: 05/09/13). P1–P9 represent point elevation measurement locations. During jökulhlaups: (a) 11 March – 17 April 2010; (b) 17 April – 08 May 2010. Following jökulhlaup deposition: (c) 08 May – 10 July 2010; (d) 10 July 2010 – 05 September 2013; (e) 05 September 2013 – 01 October 2016.

2010 jökulhlaups (Table 1). This value is ∼1.5 times greater than that initially calculated by Dunning and others (2013). The volume of deposit remaining in the basin as of 1 October 2016 is calculated to be 19.8×10^6 m^3, implying a volumetric loss of 6.0×10^6 m^3 since emplacement of the jökulhlaup deposits.

Rates of elevation change between 2010 and 2016 vary both spatially and temporally (Fig. 6). At all point measurement locations, surface elevations reach maxima after the jökulhlaups ceased following the termination of the eruption (i.e. 11 May 2010). Erosion and degradation of the sediments deposited from the largest jökulhlaups on 14–16 April 2010 occurred at several locations across the basin (i.e. P1, P3, P7 and P9). However, the overall net elevation increase of the deposits throughout the basin indicates the jökulhlaups were generally constructional until at least 11 May 2010 (Fig. 6). A significant reduction in

elevation occurred throughout the basin between 11 May and 10 July 2010, with lowering ranging between 2 and 6 m. Following this initial rapid surface elevation loss, rates of change within ice-distal locations of the basin declined over a 5-year period (based upon our data points), ranging between −0.17 and −0.45 m a^{-1} from July 2010 to June 2015. This is in contrast to the rapid reduction in surface elevation within the main channel in the ice-proximal region, with rates of up to −3.05 m a^{-1} between 2010 and 2015 (i.e. P7 and P9 in Fig. 6). The elevation of the ice-proximal fan (P8 in Fig. 6) appears to be stable for the entire period between July 2010 and October 2016, with elevation changes of less than 1 m. Lowering between 2013 and 2016 within ice-proximal regions is often associated with localised kettle hole development. This indicates the localised presence of ice within the ice-proximal deposits, although this ice is less laterally

Table 1. Volumetric change of jökulhlaup deposits within the Gígjökull basin

Date	Volumetric change (×10⁶ m³)	Volume above pre-jökulhlaup basin morphology (×10⁶ m³)
17 April 2010	19.9	19.9
08 May 2010	5.9	25.8
10 July 2010	−1.6	24.2
05 September 2013	−3.0	21.2
01 October 2016	−1.4	19.8

extensive than in the ice-distal parts of the basin. Between 2015 and 2016, surface lowering became more pronounced in distal portions of the basin, with rates increasing from an average of −0.33 m a^{-1} (2010–2015) to an average of −1.88 m a^{-1} (2015–2016) (Fig. 6).

Sub-surface reconstruction

Analysis of radargrams acquired within the Gígjökull basin enables characterisation of the 3D geometry of sub-surface sedimentary units (Fig. 7). Observations from the radargrams show that the spatial extent of reflections related to a series of distinct sub-surfaces (SS1–SS5) varies from ice-proximal to ice-distal locations. Sub-surfaces SS1 to SS4 are interpreted to delimit the primary boundaries between four major sedimentary units deposited during the 2010 jökulhlaups. We interpret the base of the 2010 jökulhlaup

sedimentary succession, and thus the former proglacial lake bed, as SS4. This is suggested based on the consistency of the GPR velocity-determined elevation of SS4 with aggradation levels calculated by Dunning and others (2013). SS5 lacks sufficient coherency for a conclusive interpretation, but it is suggested to be a reflection from an interface below the base of jökulhlaup sedimentation. The reflections associated with the surfaces SS1 and SS2 are clearly apparent within the ice-proximal fan deposits but cannot be traced beyond the perimeter of the fan (Fig. 7). As a result of their reduced extent, we believe these units are a product of the later smaller jökulhlaups that inundated the Gígjökull basin (20 April 2010 to 16 May 2010). Both SS3 and SS4 can be seen at their greatest depths under the ice-proximal fan and decrease in depth as they are traced towards the ice-distal margins of the deposits. The sediment units located below SS2 were likely deposited during the largest jökulhlaups (14–16 April 2010) based upon their spatial extent and the overall thickness of the sediment package (Fig. 7). The thickness of the individual sediment units can be seen to vary as surfaces are traced in the flow-parallel direction, but show a mostly uniform thickness when analysed perpendicular to flow (Fig. 7c). The overall thickness of the jökulhlaup deposits within the Gígjökull basin decreases in the direction of jökulhlaup flow, ranging from 67 m ice-proximally to 6.9 m in ice-distal locations (Fig. 7b). Deposit thickness remains relatively uniform when viewed transverse to flow (Fig. 7c). Post-depositional meltout structures are visible within GPR data, exemplified by trough-like structures surrounded by chaotic and high angle dipping reflections, associated with subsidence and degradation of the sediments (Fig. 7). However, the overall chaotic nature of the reflections and the low frequency of the GPR system used makes identification difficult.
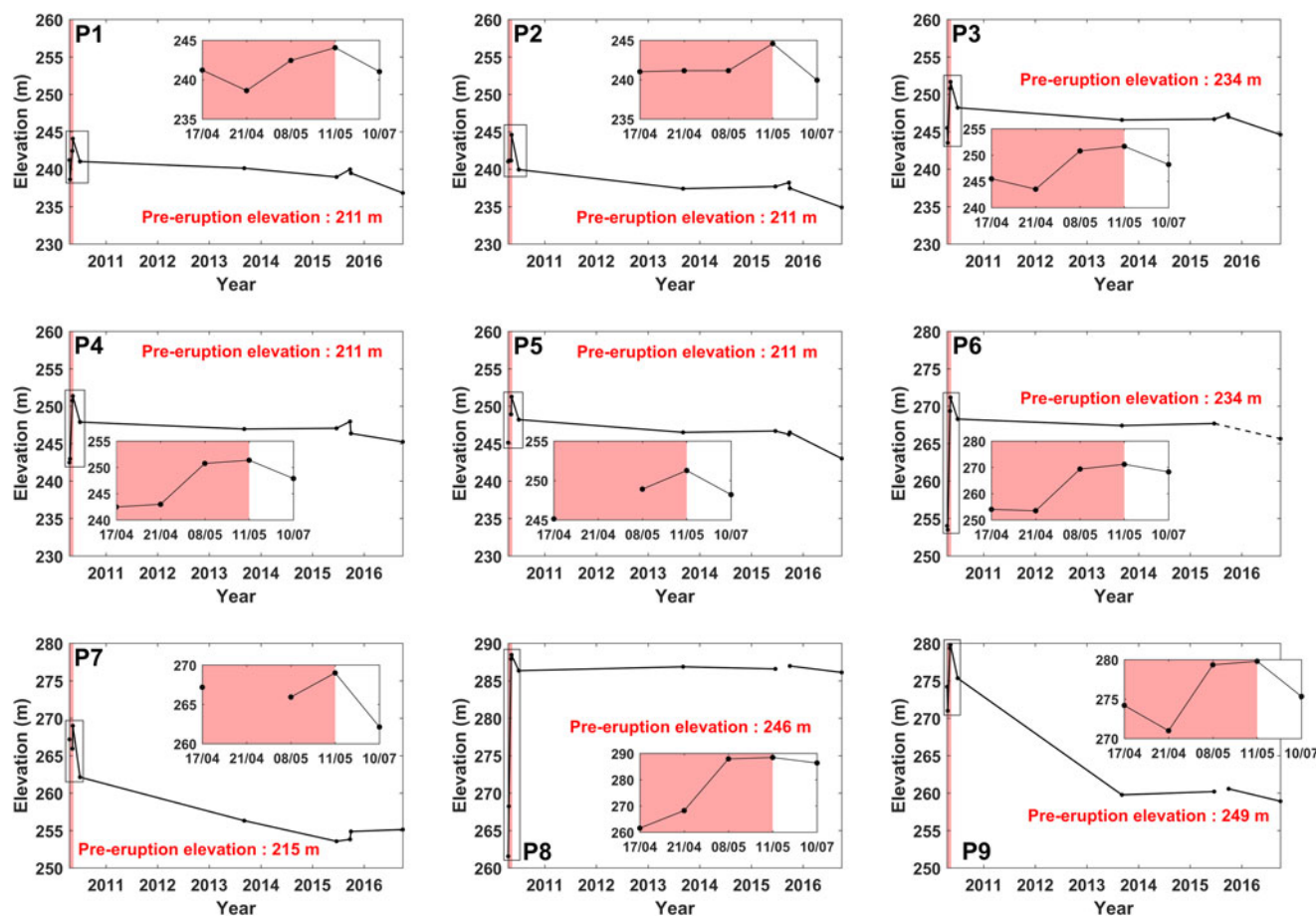

Fig. 6. Point elevation change measurements 17 April 2010 – 01 October 2016 taken from TLS, dGPS and ArcticDEM datasets. Point locations shown in Fig. 1. Red shaded region indicates the time period associated with the 2010 jökulhlaups (14 April to the 16 May).
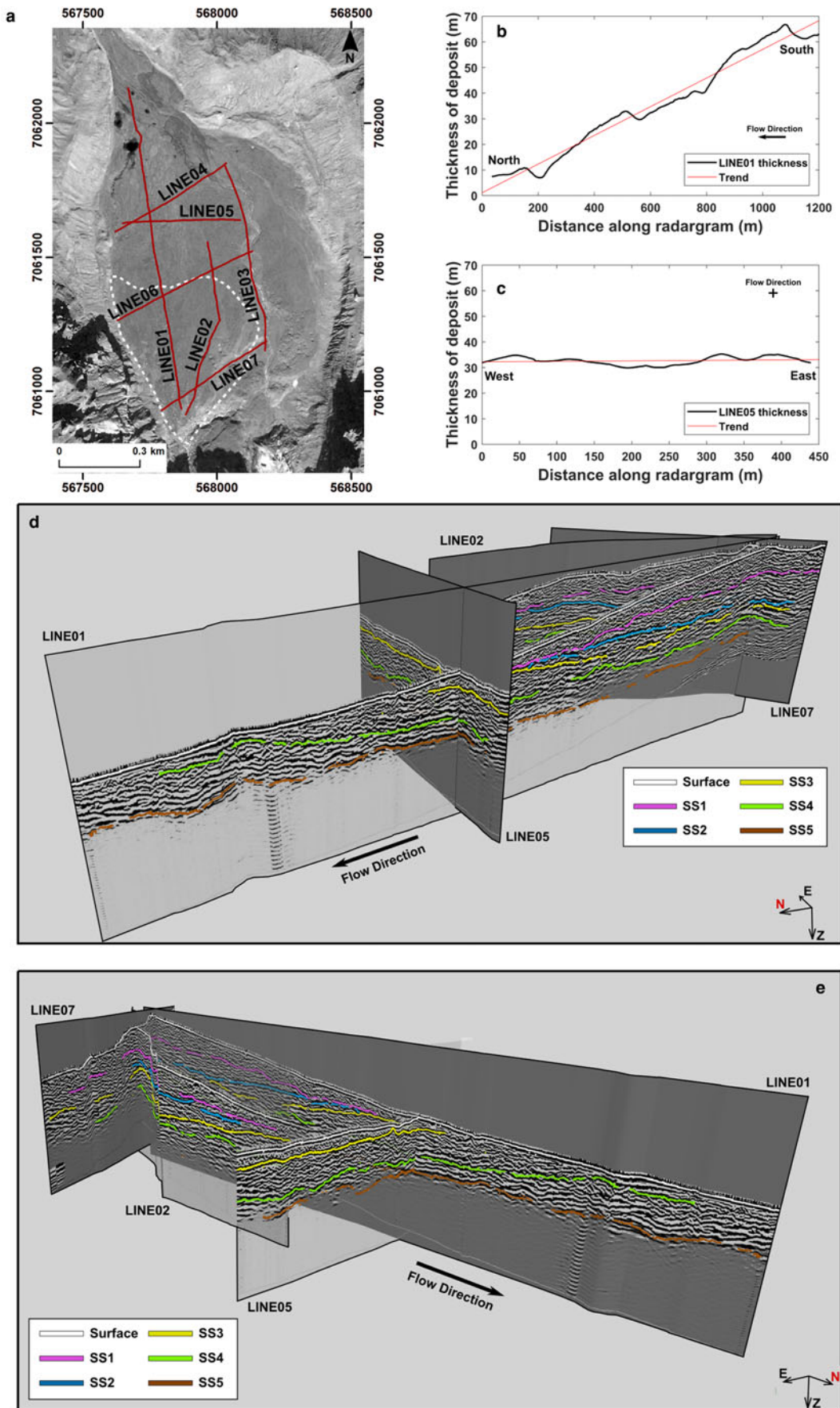
Fig. 7. Sub-surface geometry of the Gígjökull deposits. (a) Map showing location of radar lines. (b and c) Thickness of jökulhlaup deposit acquired from Line01 (b) and Line05 (c). (d and e) 3D grid of radargrams highlighting sediment units and their bounding surfaces.
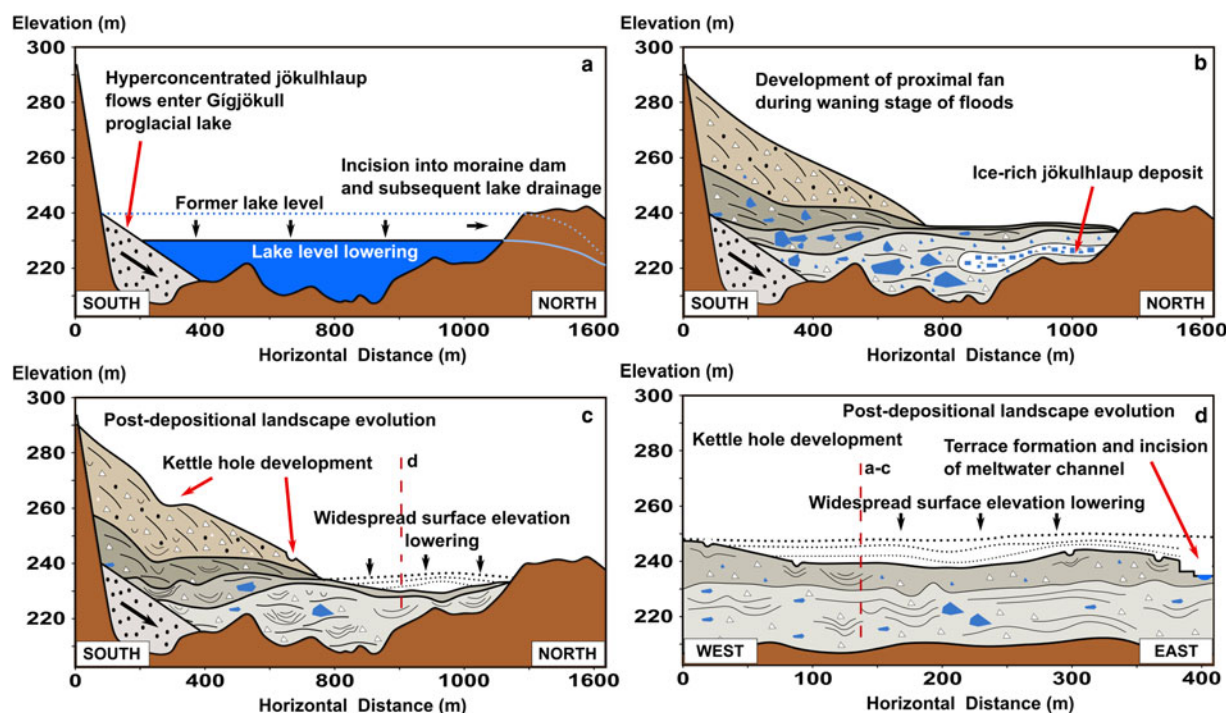
Fig. 8. Schematic model of the Gígjökull basin evolution following deposition from multiple jökulhlaups. Grey coloured deposits related to observed GPR units in Figure 7. (a) Deposition of jökulhaup sediments into proglacial water body during 14 April 2010 jökulhlaup (Dunning and others, 2013). (b) Development of large jökulhaup deposit and emplacement of an ice-rich deposit in distal locations. Blue polygons represent ice-rich deposits (i.e. not an exact location of buried ice). (c and d) Post-jökulhlaup modification related to meltout of buried ice masses and fluvial incision.

Discussion

We attribute elevation lowering of the jökulhlaup deposits in the Gígjökull basin between 2010 and 2016 to three primary factors: (i) the meltout of ice deposited by the jökulhlaups; (ii) rapid melting of the buried Gígjökull terminus following the 2010 jökulhlaups; and (iii) incision of the proglacial fluvial system into the deposits.

Meltout of buried ice

Meltout of subsurface ice is the most likely cause of the overall surface lowering of the Gígjökull deposits between 2010 and 2016. This is consistent with the presence of active ice melt and kettle hole formation within the basin during this period. It is known that deposits from the 15 April 2010 jökulhlaup (GPR unit between SS3 and SS4) consisted of up to 80% ice (Magnússon and others, 2012; Dunning and others, 2013). Ice was deposited within the Gígjökull basin in the form of large ice blocks and sediment-rich ice slurries (Dunning and others, 2013). The pattern of surface lowering over time indicates that ice melt does not occur at a uniform rate across the basin, and is likely controlled by multiple factors (e.g. distribution of ice, variations in temperature, thickness of overburden). Spatially, the surface lowering attributed to ice melt is predominately located within ice-distal regions (Fig. 5), compared to the limited or localised surface lowering due to ice melt in ice-proximal areas. Ice-proximal meltout is attributed to the rapid melting of the buried Gígjökull terminus immediately following jökulhlaup deposition (Fig. 4 and P9 in Fig. 6) and meltout of individual ice blocks deposited during the later, smaller magnitude, less ice-rich jökulhaups. In contrast, surface elevation changes observed across wide areas of the distal portions of the Gígjökull basin are consistent with the meltout of a spatially extensive ice-rich jökulhlaup deposit (GPR unit between SS3 and SS4) (Fig. 8). The 15 April jökulhlaup consisted of an ice-rich slurry, which was observed

flowing across the entire Gígjökull basin (Dunning and others, 2013). This deposit had a thickness of at least 8 m based on the total amount of surface lowering in ice-distal locations (Fig. 8). In addition to the meltout of ice within the 2010 jökulhlaup deposits, there is also potential that ice-distal surface lowering could be due to the meltout of buried glacier ice at depth. The terminus of Gígjökull was located in the ice-distal parts of the basin as recently as 1994 (Kirkbride and Dugmore, 2008). The spatial variations in surface elevation change shown in Figure 5 are interpreted to be the result of the ice-proximal to ice-distal tapering of deposit thickness (Fig. 7). Where the thickness of jökulhlaup sediment is greatest (i.e. beneath the proximal fan deposited by the later jökulhlaups between 20 April 2010 and 16 May 2010) (Fig. 7), there was little surface elevation change (2013–2016). In contrast, where the ice-slurry rich deposits associated with the 15 April jökulhlaups are closest to the surface (i.e. in ice-distal parts of the basin beyond the proximal fan), we observed high rates of surface lowering (2013–2016). This interpretation is consistent with evidence of deposit thickness influencing the ablation rates of buried ice masses elsewhere in southern Iceland (Price, 1971; Everest and Bradwell, 2003).

The volume of the jökulhlaup deposit within the Gígjökull basin decreased by 0.95×10^6 m^3 a^{-1} (~16% per year) between May 2010 and October 2016 (Table 1). This is similar to the largest rate of post-jökulhlaup volumetric change (0.6 to 0.98×10^6 m^3 a^{-1}) estimated at Mýrdalssandur in the 61 years between 1946 and 2007 (Duller and others, 2014). Duller and others (2014) attributed surface lowering at Mýrdalssandur to subterranean groundwater channels, removing volcanic material by tranquil subsurface water flow. However, an alternative interpretation is that melt of buried ice over short timescales could have been a more important process at Mýrdalssandur than previously thought, particularly given the potential for high volumes of ice to be transported during jökulhlaups over Mýrdalssandur (Russell and others, 2009).

Fluvial incision and terrace formation

Incision of the Gígjökull deposits began as early as 4 May 2010 (Dunning and others, 2013), before the series of jökulhlaups had ended, with incision into ice-proximal deposits at the foot of the gorges and subsequent terrace formation (Fig. 3). Observations from July 2010 show that the meltwater stream emanating from the gorges rapidly occupied the space left by the rapid melting of the buried glacier margin. Further fluvial incision and terrace formation (July 2010 to September 2016) within the deposits led to the dissection of the deposit surface that was documented immediately post-eruption (Dunning and others, 2013). Incision into jökulhlaup deposits during post-flood lower magnitude fluvial activity is common in proglacial environments that have undergone aggradation from an outburst flood (Russell and others, 2009), and is one of many documented processes that occur in a glacio-volcanic outwash environment (Maizels, 1997). Elevation data (TLS-derived DEM from July 2010) indicate fluvial incision, and meltwater system development at Gígjökull can be seen to occur roughly 1 month following deposition, and is well developed by September 2013 (Fig. 5). This is consistent with the theory that incision and terrace formation into jökulhlaup deposits occurs rapidly after the jökulhlaups have ended (Marren and Toomath, 2013). The fluvial incision at Gígjökull is likely a result of an overall reduction in sediment supply since the end of the 2010 Eyjafjallajökull eruption and the fluvial system regrading along its long profile (Mackin, 1948; Schumm, 1979). Although the meltwater system has played a crucial role in the post-jökulhlaup geomorphic evolution of the Gígjökull basin, the meltout of buried ice masses (e.g. glacier ice, large ice blocks and small ice fragments) is believed to be the primary factor in determining the post-deposition evolution of the landscape.

Conclusions and wider implications

Analysis of geodetic data spanning from 2010 to 2016 has provided a comprehensive quantification of post-depositional surface-elevation change, and an assessment of the role of buried glacier ice in the post-depositional evolution of a jökulhlaup sandur. This study has quantified post-deposition rates of volumetric change within the Gígjökull basin of up to -1×10^6 m^3 a^{-1}. Rates of surface lowering vary between proximal and distal locations and increase between 2015 and 2016. Combining the surface elevation change data with GPR profiles has allowed for the development of a schematic model displaying post-jökulhlaup landscape response as a result of ice-laden jökulhlaup flows (Fig. 8). Post-depositional meltout of buried ice masses is the dominant process in surface lowering within the Gígjökull basin. The presence of post-depositional meltout structures within the subsurface of the deposits, the development of kettle holes throughout the Gígjökull basin and the nature of the surface lowering provide the supporting evidence for this interpretation. Proximal-to-distal variation in surface lowering is attributed to a thicker sediment body in ice-proximal locations insulating buried, jökulhlaup deposited ice. The uniform and rapid reduction in elevation in ice-distal locations is believed to reflect the degradation of the ice-rich 15 April 2010 jökulhlaup deposit. These results indicate that significant surface subsidence related to buried ice meltout can occur for at least 6 years following the emplacement of an ice-rich jökulhlaup deposit. This study has characterised the nature of surface lowering related to buried ice meltout and evaluated the role of ice in the development of jökulhlaup deposits. Further geophysical investigations (e.g. electrical resistivity tomography) are required to quantify and map out the locations and structure of buried ice masses.

References

Arun PV (2013) A comparative analysis of different DEM interpolation methods. *Egypt. J. Remote Sens. Space Sci.*, **16**(2), 133–139 (doi: 10.1016/j.ejrs.2013.09.001)

Björnsson H (2002) Subglacial lakes and jökulhlaups in Iceland. *Glob. Planet. Change*, **35**(3–4), 255–271 (doi: 10.1016/S0921-8181(02)00130-3)

Burke MJ, Woodward J and Russell AJ (2010) Sedimentary architecture of large-scale, jökulhlaup-generated, ice-block obstacle marks: examples from Skeiðarársandur, SE Iceland. *Sediment. Geol.*, **227**(1–4), 1–10 (doi: 10.1016/j.sedgeo.2010.03.001)

Carrivick JL and 6 others (2009) Geomorphological evidence towards a de-glacial control on volcanism. *Earth Surf. Proc. Land.*, **34**(8), 1164–1178 (doi: 10.1002/esp.1811)

Cassidy N (2003) GPR derived architecture of November 1996 jökulhlaup deposits, Skeiðarársandur, Iceland. *Geol. Soc. Spec. Publ.*, **211**, 153–166 (doi: 10.1144/GSL.SP.2001.211.01.13)

Dai C and Howat I (2017) Measuring Lava Flows With ArcticDEM: application to the 2012–2013 Eruption of Tolbachik, Kamchatka. *Geophys. Res. Lett.*, **44**, 12133–12140 (doi: doi.org/10.1002/2017GL075920)

Duller RA and 5 others (2014) Landscape reaction, response, and recovery following the catastrophic 1918 Katla jökulhlaup, southern Iceland. *Geophys. Res. Lett.*, **41**, 4214–4221 (doi: 10.1002/2014GL060090.Received)

Duller R, Mountney N, Russell A and Cassidy N (2008) Architectural analysis of a volcaniclastic jökulhlaup deposit, southern Iceland: sedimentary evidence for supercritical flow. *Sedimentology*, **55**(4), 939–964 (doi: 10.1111/j.1365-3091.2007.00931.x)

Dunning SA and 8 others (2013) The role of multiple glacier outburst floods in proglacial landscape evolution: the 2010 Eyjafjallajökull eruption, Iceland. *Geology*, **41**(10), 1123–1126 (doi: 10.1130/G34665.1)

Everest J and Bradwell T (2003) Buried glacier ice in southern Iceland and its wider significance. *Geomorphology*, **52**(3–4), 347–358 (doi: 10.1016/S0169-555X(02)00277-5)

Fay H (2002a) Formation of Ice-Block Obstacle Marks during the November 1996 Glacier-Outburst Flood (Jökulhlaup), Skeiðarársandur, Southern Iceland. Flood and Megaflood Processes and Deposits, 85–97.

Fay H (2002b) Formation of kettle holes following a glacial outburst flood (Jökulhlaup), Skeiðarársandur, southern Iceland. *Extremes of the Extremes: Extraordinary Floods*, **271**(271), 205–210.

Francke J and Utsi V (2009) Advances in long-range GPR systems and their applications to mineral exploration, geotechnical and static correction problems. *First Break*, **27**(JULY), 85–93.

Harrison D (2018) *Geomorphic Evolution of the Gígjökull Basin.* (M.Phil. thesis, Newcastle University)

Kirkbride MP and Dugmore AJ (2008) Two millennia of glacier advances from southern Iceland dated by tephrochronology. *Quat. Res.*, **70**(3), 398–411 (doi: 10.1016/j.yqres.2008.07.001)

Mackin JH (1948) Concept of the graded river. *Bull. Geol. Soc. Am.*, **59**, 463–511 (doi: 10.1130/0016-7606(1948)59[463:COTGR]2.0.CO;2)

Magnússon E and 5 others (2012) Ice-volcano interactions during the 2010 Eyjafjallajökull eruption, as revealed by airborne imaging radar. *J. Geophys. Res. Solid Earth*, **117**(7), 1–17 (doi: 10.1029/2012JB009250)

Maizels JK (1992) Boulder Ring Structures Produced During Jökulhlaup Flows: origin and hydraulic significance. *Geogr. Ann. Ser. A Phys. Geogr.*, **74**(1), 21–33 (doi: 10.2307/521467)

Maizels JK (1997) Jökulhlaup deposits in proglacial areas. *Quat. Sci. Rev.,* **16**(7), 793–819 (doi: 10.1016/S0277-3791(97)00023-1)

Marren PM and Toomath SC (2013) Fluvial adjustments in response to glacier retreat: Skaftafellsjökull, Iceland. *Boreas,* **42**(1), 57–70 (doi: 10.1111/j.1502-3885.2012.00275.x)

Noh MJ and Howat IM (2015) Automated stereo-photogrammetric DEM generation at high latitudes: Surface Extraction with TIN-based Search-space Minimization (SETSM) validation and demonstration over glaciated regions. *GISci. Remote Sens.,* **52**(2), 198–217 (doi: 10.1080/15481603.2015.1008621)

Pagli C and Sigmundsson F (2008) Will present day glacier retreat increase volcanic activity? Stress induced by recent glacier retreat and its effect on magmatism at the Vatnajökull ice cap, Iceland. *Geophys. Res. Lett.,* **35**(9), 3–7 (doi: 10.1029/2008GL033510)

Porter C and 28 others (2018) ArcticDEM (doi: 10.7910/DVN/OHHUKH).

Price RJ (1971) The development and destruction of a sandur, Breiðamerkurjökull, Iceland. *Arct. Alp. Res.,* **3**(3), 225–237 (doi: 10.2307/1550195)

Reynolds JM (2011) *An Introduction to Applied and Environmental Geophysics,* 2nd edn. Wiley-Blackwell, Chichester.

Ross N, Sole A, Livingstone S, Igneczi A and Morlighem M (2018) Near-margin ice thickness from a portable radar: implications for subglacial water routing, Leverett Glacier, Greenland. *Arct. Antarct. Alp. Res.,* **50**(1), S100007 (doi: 10.1080/15230430.2017.1420949)

Russell A and 6 others (2010) An unusual jökulhlaup resulting from subglacial volcanism, Sólheimajökull, Iceland. *Quat. Sci. Rev.,* **29**(11–12), 1363–1381 (doi: 10.1016/j.quascirev.2010.02.023)

Russell A, Duller R and Mountney N (2009) 11 Volcanogenic Jökulhlaups (Glacier Outburst Floods) from Mýrdalsjökull: impacts on proglacial environments. *Dev. Quat. Sci.,* **13**, 181–207 (doi: 10.1016/S1571-0866(09)01311-6)

Schumm SA (1979) Geomorphic thresholds: the concept and its applications. *Trans. Inst. Br. Geogr.,* **4**(4), 485–515. ISSN 00202754 (doi: 10.2307/622211)

Sigurðsson O, Williams RS and Víkingsson S (2017) *Map of the Glaciers of Iceland,* 2nd edn. Ved. h. urstofa Íslands, Reykjavík.

Snorrason A (2012) Floods in iceland. In Kundzewicz ZW ed. *Changes in flood risk in Europe,* CRC Press, Florida, 257–276.

Spedding N (2000) Hydrological controls on sediment transport pathways: implications for debris-covered glaciers. *Debris-covered Glaciers: Proceedings of an International Workshop Held at the University of Washington in Seattle, Washington, USA, 13–15 September 2000,* (264), 133–142.

Sturkell E and 6 others (2010) Katla and Eyjafjallajökull Volcanoes. *Dev. Quat. Sci.,* **13**, 5–21 (doi: 10.1016/S1571-0866(09)01302-5)